

UCRL-JC--105032

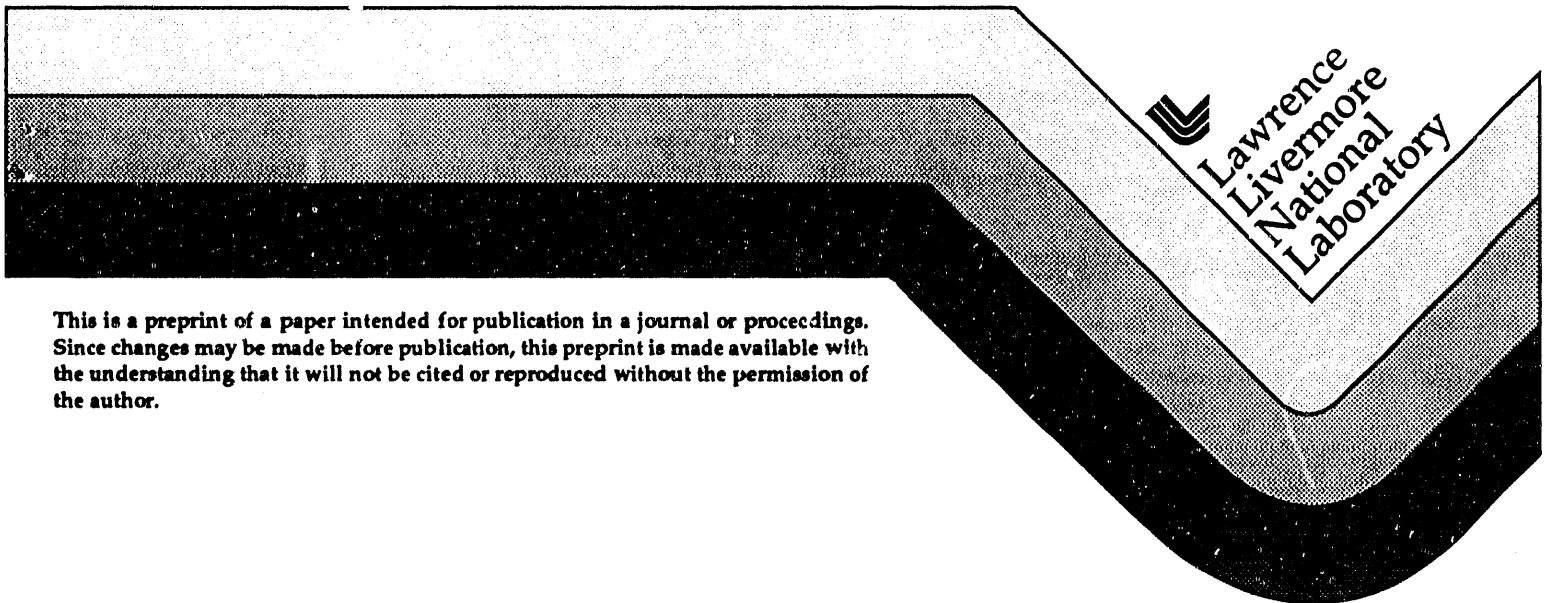
DE91 007344

Short Wavelength Nickel-Like X-Ray Laser Development

B. MacGowan, L. DaSilva, D. Fields, A. Fry, C. Keane,
J. Koch, D. Matthews, S. Maxon, S. Mrowka,
A. Osterheld, H. Scofield and G. Shimkaveg

This paper was prepared for submittal to the
Proceedings of the 2nd Int'l Colloquium,
York, England,
Septemer 16-21, 1990

January 7, 1991



This is a preprint of a paper intended for publication in a journal or proceedings. Since changes may be made before publication, this preprint is made available with the understanding that it will not be cited or reproduced without the permission of the author.

MP

MASTER

DISTRIBUTION OF THIS DOCUMENT IS UNLIMITED

DISCLAIMER

This document was prepared as an account of work sponsored by an agency of the United States Government. Neither the United States Government nor the University of California nor any of their employees, makes any warranty, express or implied, or assumes any legal liability or responsibility for the accuracy, completeness, or usefulness of any information, apparatus, product, or process disclosed, or represents that its use would not infringe privately owned rights. Reference herein to any specific commercial products, process, or service by trade name, trademark, manufacturer, or otherwise, does not necessarily constitute or imply its endorsement, recommendation, or favoring by the United States Government or the University of California. The views and opinions of authors expressed herein do not necessarily state or reflect those of the United States Government or the University of California, and shall not be used for advertising or product endorsement purposes.

Short wavelength nickel-like x-ray laser development

B.J. MacGowan, L.B. Da Silva, D.J. Fields, A. R. Fry, C. J. Keane;
J.A. Koch, D. L. Matthews, S. Maxon, S. Mrowka, A. L. Osterheld,
J. H. Scofield, and G. Shimkaveg

*Lawrence Livermore National Laboratory, University of California,
L-483, P.O. Box 808, Livermore, California 94550, U.S.A.*

ABSTRACT: Ni-like x-ray lasers have been produced at wavelengths near to, and below the carbon K edge (43.76-Å). Recent work has concentrated on the development of the Ni-like Ta amplifier at 44.83-Å. Amplification occurs in a laser produced plasma created by irradiating a thin foil of Ta with two beams of the Nova laser. Up to 8 gainlengths have been demonstrated so far, with a gain coefficient of 3.2 cm^{-1} and a gain duration of 250 psec. The wavelength of 44.83-Å is close to optimal for holographic imaging of live cells. It remains to optimize the coherent output power of the amplifier to use it as a source for future x-ray holography experiments.

Nickel-like x-ray lasers¹⁻⁶ are 4d - 4p transitions in ions isoelectronic to Ni-I. Laser action occurs as the 4d levels are metastable to radiative decay to the 3d¹⁰ Ni-like ground state, while the 4p levels rapidly decay back to the ground state. Ni-like 3d⁹4d - 3d⁹4p lasers are direct analogues of the 2p⁵3p - 2p⁵3s laser transitions in neon-like ions that were first demonstrated in a laser produced plasma of Ne-like selenium in 1984.^{7,8} and subsequently extrapolated to shorter wavelength⁹. Ni-like x-ray lasers were first demonstrated in 1987 in a laser produced plasma of Eu³ when four gainlengths of amplification were observed at 71.0-Å. Subsequently the scheme was isoelectronically extrapolated to 43.18-Å in Ni-like W⁶ and 35.6-Å in Ni-like Au. One motivation for the development of short wavelength Ni-like lasers was the goal of producing a coherent, high brightness source suitable for holography of biological specimens within the "water window" between the K edges of carbon and oxygen¹⁰. A recent study of the power required for x-ray holographic imaging, by London et al¹¹ has shown that for x-ray holography^{10,12} the x-ray dosage received by a cell is minimized for a given image resolution if the illumination wavelength is slightly to the long wavelength side of the carbon K edge. The Ni-like Ta amplifier at 44.83-Å lies at the edge of the water window, and is a potential x-ray source that could fulfill some of the requirements for holography of living cells.

The Ni-like laser scheme is illustrated for Ni-like Ta in Fig. 1 which shows the

4d - 4p laser transitions predicted to have the highest gain. The 4d levels are populated through a combination of direct collisional excitation from the ground state and cascading from upper levels. The 4d - 4p population inversion is maintained by fast radiative decay from the 4p levels to the ground state. Several transitions are capable of being inverted, but the largest gain is observed on the 44.83-Å J = 0 - 1 transition $3d_{3/2}4d_{3/2}0 - 3d_{3/2}4p_{1/2}1$. The upper state is pumped predominantly (over 90%) by collisional excitation from the $3d^{10}$ ground state. Other transitions predicted to have large gain^{2,4} include a second J = 0 - 1 transition (at 50.97-Å), a J = 2 - 1, and a J = 1 - 1 4d - 4p transition. In experiments, Ni-like lasers show significant gain only on the J = 0 - 1 transitions while the J = 2 - 1 and 1 - 1 lines have little or no gain. This observation is the opposite of experience with Ne-like lasers where high angular momentum transitions were found to have the highest gain. The second, longer wavelength J = 0 - 1 transition has more gain in lower-Z ions³ but in higher-Z ions its shorter wavelength partner becomes dominant¹³.

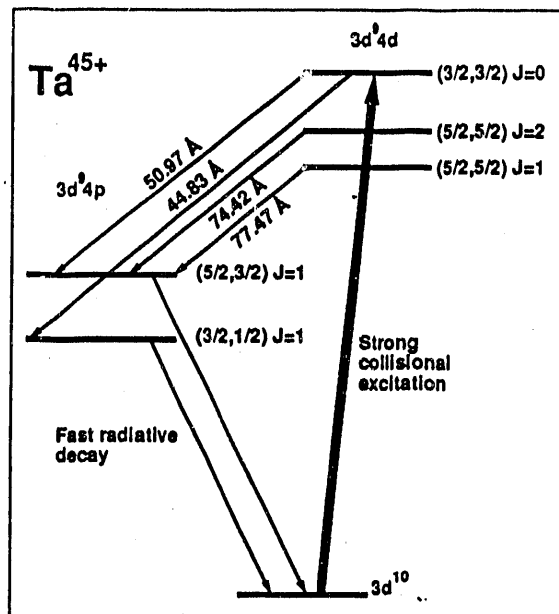


Figure 1. Simplified energy level diagram for Ni-like Ta showing the four 4d - 4p transitions most likely to be amplified.

Experiments with Ni-like Ta lasers have the aim of producing a laser at the edge of the water window. The Ni-like Ta amplifier is produced by irradiating a thin foil of Ta with a high intensity optical laser, heating the foil and producing a plasma that expands to form a large, uniform gain medium. The first successful experiments with Ni-like Ta⁶ used a foil of $127 \mu\text{gcm}^{-2}$ Ta on a $24 \mu\text{gcm}^{-2}$ Lexan substrate, irradiated simultaneously with two beams of the Nova laser. The line focused beams ($120 \mu\text{m}$ by up to 2 cm) were superposed with a total irradiance of $4.6 \cdot 10^{14} \text{ Wcm}^{-2}$. The 2ω pulse was a 500 psec (full width at half power) gaussian. The foil was set up in a target chamber vacuum vessel with a large number of XUV and x-ray spectrometers and imaging diagnostics. The foil was viewed from one end of its axis (the preferred direction for stimulated emission) by a gated grazing incidence XUV spectrometer with a micro-channel plate detector (the MCPIGS) and from the other end by a flat field grating spectrometer linked to an x-ray streak camera (the SFFS). Another MCPIGS spectrometer viewed the plasma from an off-axis direction while various time resolved and time integrated x-ray spectrometers recorded the 5 - 3 x-ray transitions as an indication of the charge state of the plasma.

The on-axis spectra were dominated by strong line emission at 44.83-Å; weaker Ni-like emission was visible at 50.97, 74.42, and 77.47-Å and identified as the transitions shown in Fig. 1. Gain of 2.3 cm⁻¹ was measured on the 44.83-Å J = 0 - 1 line⁶. In the same experiment, W foils of nominal thickness 89 μgcm⁻² on 20 μgcm⁻² Lexan, up to 3 cm in length, were irradiated with a total of 3.2 10¹⁴ Wcm⁻² of 2ω light. Tungsten was studied as it is the element next to Ta in the periodic table, and its behavior was expected to be similar. Figure 2(a) shows on-axis MCPIGS spectra from 2.5 and 1.7 cm long W foils with the J = 0 - 1 laser line at 43.185-Å in 1st and 2nd order and weaker J = 2 - 1 and J = 1 - 1 Ni-like lines at 72.40 and 75.35-Å respectively. In Fig. 2(b) the intensity of the 43.185-Å line is plotted as a function of foil length. The time integrated gain is 2.6 cm⁻¹ with a maximum gainlength of 7 recorded. The gains measured for other lines in Ni-like W were consistent with those measured for Ta⁶.

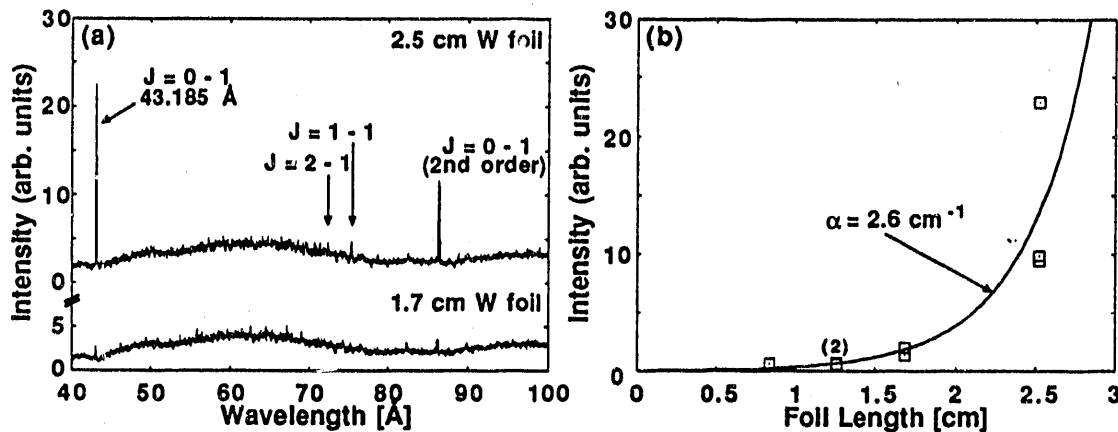


Figure 2. (a) On axis spectra from 2.5 and 1.7 cm long W foils. The 2.5 cm foil had a gainlength product of 7 on the 43.18-Å J = 0 - 1 laser line. (b) Intensity of the 43.18-Å J = 0 - 1 transition of Ni-like W as a function of foil length. The fit is to the equation: $I = (\epsilon/\alpha)(e^{\alpha l} - 1)^{1.5}(\alpha l e^{\alpha l})^{-0.5}$ for a distributed source with emissivity ϵ , small signal gain α and length l ¹⁴. Reproduced with permission from Ref 6. Copyright 1990, The American Physical Society.

Subsequent to the W experiment described in Ref. 6, two shots were fired with the SFFS configured to time resolve the W laser emission. The result is illustrated in Fig. 3 which shows a lineout of the time history of the W 43.185-Å laser line. The streaked flat field spectrometer (SFFS) is a Harada grating¹⁵ spectrometer coupled to an x-ray streak camera with 40 psec continuous time resolution. This data was recorded from a 2.5 cm target that produced a similar MCPIGS spectrum to that seen in the first W experiments. The data

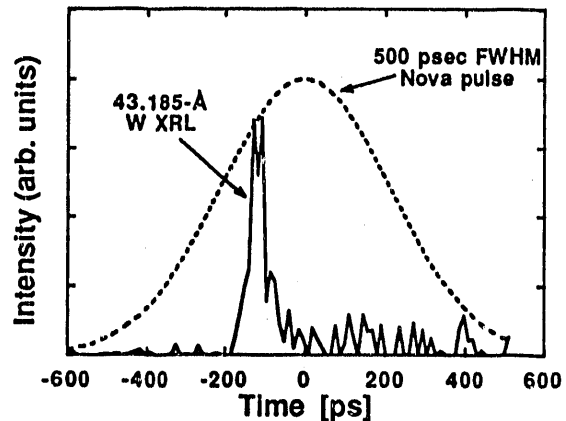


Figure 3. Time history of the on-axis 43.18-Å laser emission from a 2.5 cm long W target. The dashed curve represents the time history of the 500 psec gaussian Nova pulse.

is a lineout of the 3rd order spectrum and illustrates the short time duration (60 - 70 psec full width at half power) of the laser emission and that it occurs well before the peak of the Nova pulse as determined using an optical timing fiducial¹⁶. The Ta experiment of Ref. 6 showed Ta laser durations of order 300 psec and actually time resolved the gain through making fits to the formula of Ref. 14 at different times on the streaked SFFS data. The gain time duration was found to be 250 psec for the Ta amplifiers. Therefore there is an inconsistency which may be explained by the W targets being thinner than we thought and hence burning through more rapidly. This, and other possible causes of the short time duration of the W x-ray laser are being investigated.

The first Ta experiments, and also Yb experiments carried out at the same time, were notable as they were the first experiments where cobalt-like laser lines were observed¹⁷. Co-like is the next ionization state beyond Ni-like, with a ground state consisting of a vacancy in the 3d shell. Figure 4(a) shows the Ni-like Yb laser scheme for the highest gain 4d - 4p laser transition. The upper state is pumped predominantly (over 90%) by collisional excitation from the $3d^{10}$ ground state. Collisional excitation rates¹⁸ are for an electron temperature of

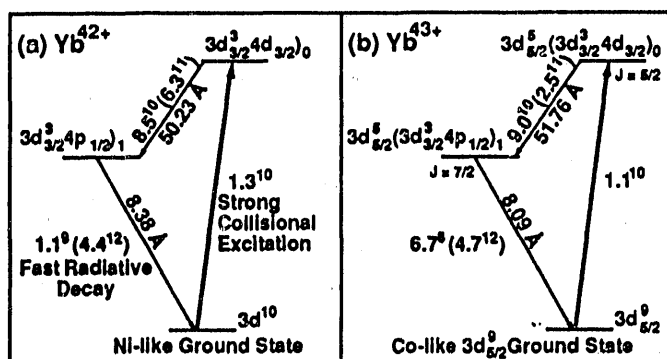


Figure 4. Simplified energy level diagram for: a) Ni-like Yb and b) the analogous levels in Co-like Yb showing the main levels communicating with the brightest 4d - 4p transition in both ions. Upward collisional rates are shown with spontaneous emission rates in parentheses.

0.8 keV and an electron density of 10^{21} cm^{-3} , representative of Ni-like Yb x-ray laser plasmas. The Co-like ground state mostly consists of $3d_{5/2}$ and $3d_{3/2}$ holes in an otherwise closed $n = 3$ shell. The Co-like analog to the Ni-like $J = 0 - 1$ laser is illustrated in Fig. 4(b). The transition is $3d_{5/2}(3d_{3/2}4d_{3/2})_0$ ($J=5/2$) - $3d_{5/2}(3d_{3/2}4p_{1/2})_1$ ($J=7/2$), the same configurations as for the brightest Ni-like line but with an extra $3d_{5/2}$ vacancy.

Figure 5 shows time resolved spectra, at the peak of the Ni-like x-ray laser emission, from the streaked spectrometer looking along the axis of Ta x-ray laser foils. The lower spectrum is from a 1.7 cm long, $127 \mu\text{gcm}^{-2}$ thick Ta foil irradiated at $4.6 \cdot 10^{14} \text{ Wcm}^{-2}$. The Ni-like x-ray laser line is evident at $44.83\text{-}\text{\AA}$, together with a Co-like satellite at $46.07\text{-}\text{\AA}$. The upper spectrum is from a 2.5 cm long, $95 \mu\text{gcm}^{-2}$ Ta foil irradiated at a lower irradiance of $2.4 \cdot 10^{14} \text{ Wcm}^{-2}$; although the Ni-like $J = 0 - 1$ is brighter the Co-like satellite has disappeared. The Co-like satellite line was also seen (at $51.76\text{-}\text{\AA}$) from Yb foils both on the SFFS and the on-axis MCPIGS. None of the Ni-like or satellite lines were visible in the off-axis MCPIGS spectra. Gain was observed on the Co-like line in both Yb and Ta¹⁷, this is to be expected as Fig. 4(b) shows a transition that can be easily inverted. The upper level of the Co-like line receives over 90% of its population from the $3d_{5/2}$ ground state through direct collisional excitation.

For equal quantities of Ni- and Co-like ions and an optically thin plasma, we would expect gains in the ratio 2:1. The time resolved Co- and Ni-like line intensities from the first Ta experiment, for several plasma lengths, were fit to the Linford scaling formula¹⁴. The 127 μgcm^{-2} thick Ta data which gave a peak gain of $2.3 \pm 0.2 \text{ cm}^{-1}$ at 44.83-Å showed a gain of $2.2 \pm 0.4 \text{ cm}^{-1}$ on the Co-like Ta line. Since the upper laser levels are populated almost exclusively by collisional excitation from the ground state with similar rates this gain ratio may be an indication that the plasma is overionized. The upper spectrum in Fig. 5 is from a lower irradiance, thinner target, which shows significant gain on the Ni-like $J = 0 - 1$ ($3.2 \pm 0.5 \text{ cm}^{-1}$) but no Co-like line. This latter experiment may have an ionization balance more optimized for ground state Ni-like. It was also noticed that the long wavelength $J = 0 - 1$ line was stronger in the higher irradiance Ta data, almost disappearing at lower irradiance. The low gain on the long wavelength $J = 0 - 1$ line is a problem in the understanding of Ni-like lasers. It may be due to a higher population in the $3d_5/24p_3/2)_1$ level than in the $3d_3/24p_1/2)_1$ level (see Fig. 1). The observation of the long wavelength $J = 0 - 1$ signal decreasing as the ionization balance becomes

more Ni-like (as inferred from the Ni- to Co-like laser ratio), is consistent with two explanations for the low long wavelength $J = 0 - 1$ gain. These are; increased $3d - 4p$ radiation trapping elevating the $3d_5/24p_3/2)_1$ population, or absorption of the long wavelength $J = 0 - 1$ line by blends of $4p - 4d$ transitions in lower ionization states (e.g. Zn-, Ga-, Ge-, As-like etc.) Both of these possibilities are being investigated.

The calculated¹⁹ and observed wavelengths of the Co-like lines are summarized in Table I. The quantity ΔE is the disagreement between the calculated and observed transition energy. It can be seen that for each element, ΔE is similar for the Ni-like and Co-like lines. This observation is consistent with the identification of the Co-like lines as the configuration interaction

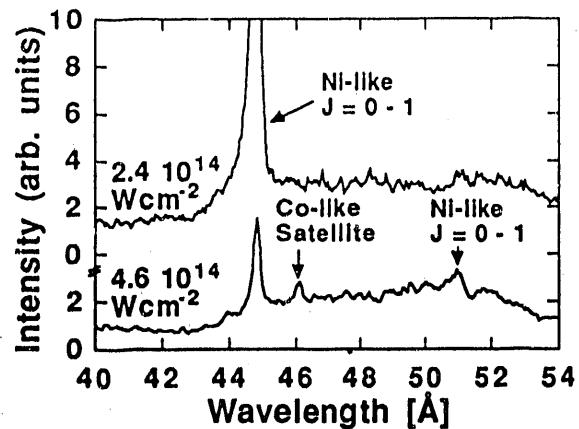


Figure 5. Time resolved on-axis spectra from Ta foils at two different irradiances illustrating that the Co-like line is stronger in the higher irradiance data.

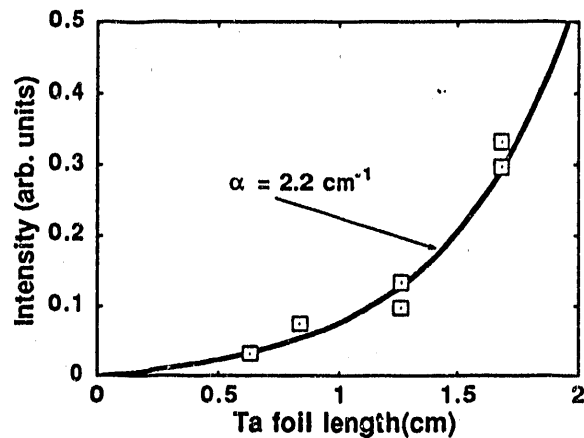


Figure 6. Measured intensity of the 46.07-Å line of Co-like Ta plotted as a function of foil length. The data are fit to the scaling formula¹⁴ for amplified spontaneous emission, for a gain of $2.2 \pm 0.4 \text{ cm}^{-1}$.

contributions to their upper level energies should be similar to those affecting the calculation of the Ni-like transition energy.

	Observed (Å)	Calculated (Å)	ΔE (eV)
Yb ⁴²⁺ Ni-like J = 0 - 1	50.23 ± 0.02	50.16	-0.34 ± 0.1
Yb ⁴³⁺ Co-like J = 5/2 - 7/2	51.71 ± 0.02	51.71	-0.23 ± 0.1
Ta ⁴⁵⁺ Ni-like J = 0 - 1	44.83 ± 0.02	44.76	-0.43 ± 0.1
Ta ⁴⁶⁺ Co-like J = 5/2 - 7/2	46.07 ± 0.02	45.97	-0.59 ± 0.1

Table I: Calculated and observed wavelengths for the Ni-like J = 0 - 1 and the analogous Co-like line.

Figure 7 shows MCPIGS spectra from 95 μgcm^{-2} Ta foils irradiated at the more optimum irradiance of $2.4 \cdot 10^{14} \text{ Wcm}^{-2}$. This experiment produced a gain of $3.2 \pm 0.5 \text{ cm}^{-1}$ on the 44.83-Å line and allowed the irradiation of 3 cm targets, to give a maximum gainlength product of 8. The SFFS time resolved spectrometer data, using the timing fiducial allowed us to compare the on-axis laser signal for different thickness Ta foils in an attempt to increase the gain. Figure 8 shows the time history of the on-axis 44.83-Å emission for a 2.5 cm long 95 μgcm^{-2} Ta foil and for a 63 μgcm^{-2} foil of the same length. The dashed curve represents the Nova heating pulse. The thicker target shows a brighter output pulse and also a longer duration. The data are consistent with the thin target burning through too early and hence producing a truncated x-ray laser pulse. Further experiments investigating the effects of target thickness and Nova pulse shape and duration are planned. This data should be compared with the W time history shown in Fig. 3, which is more consistent with that of the the 63 μgcm^{-2} Ta foil.

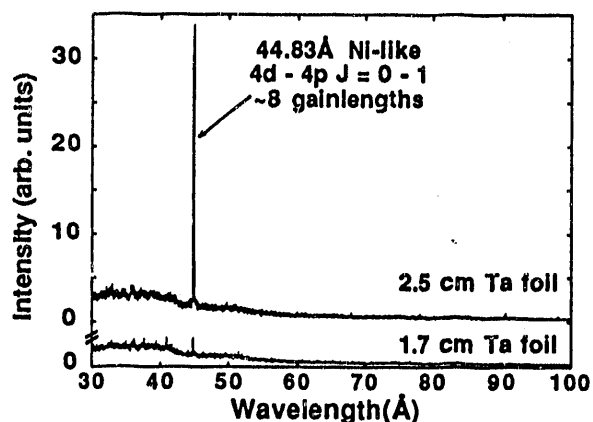


Figure 7. On-axis MCPIGS spectra from 95 μgcm^{-2} Ta targets irradiated at $2.4 \cdot 10^{14} \text{ Wcm}^{-2}$, showing ~ 8 gainlengths amplification.

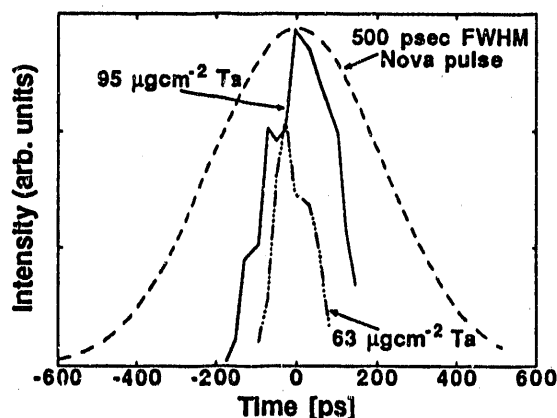


Figure 8. Time history of the on-axis 44.83-Å laser emission from 2.5 cm long Ta targets of different thickness. The Nova laser pulse is represented by a dashed curve.

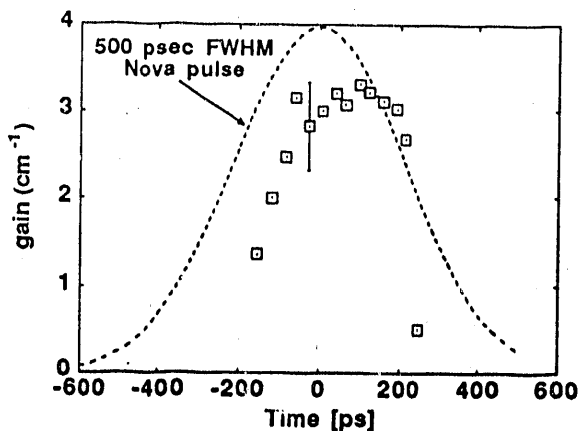


Figure 9. Time history of the gain from the $95\mu\text{gcm}^{-2}$ Ta amplifiers.

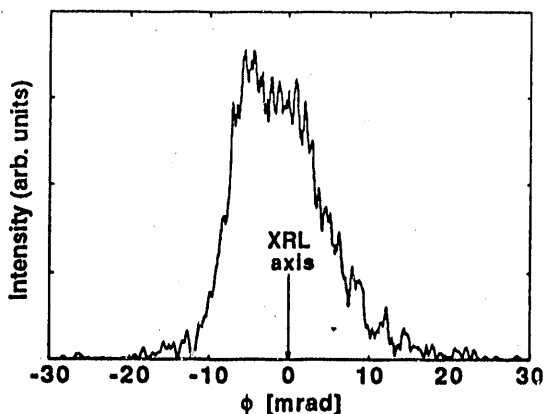


Figure 10. Horizontal divergence measured from $95\mu\text{gcm}^{-2}$ Ta foils.

Figure 9 shows the results of fits to the Linford formula for the streaked data (SFFS) from the $95\mu\text{gcm}^{-2}$ Ta amplifiers. The data from three different target lengths (1.26, 1.68 and 2.52 cm) were fit at the same times relative to the Nova pulse. The fits show a peak gain of 3.2 cm^{-1} , with an error estimated at 0.5 cm^{-1} , based on the small number of data points. The gain time history after the peak of the pulse is sensitive to the accuracy of the timing fiducial (estimated at ± 30 psec) since signals are changing so rapidly at that time. Hence the error in the gain may be higher at later time. Fits to the time integrated MCPIGS data (e.g. Fig. 7), and also integrating the SFFS data in time, gave a gain of 3 cm^{-1} . More data will be collected in the future in order to more accurately characterize the gain in this amplifier. Figure 10 shows a lineout across the MCPIGS spectrum in the direction perpendicular to the dispersion direction. The MCPIGS was modified with a pair of cylindrical grazing incidence mirrors acting as a collimator in the sagittal direction. The MCPIGS was then able to see ± 30 mrad either side of the x-ray laser axis. The data shows the amplifier to have a narrow divergence (12 mrad FWHM) in the horizontal plane, and to be almost centred on the axis with a slight offset towards the metal side of the target (negative ϕ). (The target is not quite symmetric since it has a $20\mu\text{gcm}^{-2}$ substrate of CH on one side.) This data is encouraging since it shows that the amplifier is not splitting the x-ray beam due to increased refraction at the cold ends of the target, as was seen in early experiments with Ne-like Se amplifiers. By overfilling the target, with the Nova line foci, we have therefore produced a more uniform plasma amplifier than we had in the Se experiments. The divergence in the vertical direction parallel to the initial foil surface, has not yet been measured.

The estimated energy output from a Ta amplifier of 8 gain lengths is of order $30\mu\text{J}$. The gain duration of order 250 psec is long enough to allow the use of normal incidence multilayer x-ray mirrors to double pass the gain medium. Using a 10% reflectivity mirror a net amplification equivalent to 14 gainlengths should be possible by double passing a 3 cm foil. This amplifier would have an energy output of order 1 mJ. Increasing the gain in the target through varying target and/or irradiation parameters might increase this output further. The saturation intensity of the Ta laser is estimated to be of order 10^{11} Wcm^{-2} which

would occur at 12 to 16 gainlengths (depending on the amplifier's divergence) and an energy of 4 mJ. If the divergence is restricted due to the geometry of the target or through use of apertures in combination with the mirror, the amplifier should saturate at a higher gainlength product with narrower divergence and hence be more coherent. Future experiments with Ta amplifiers will attempt to increase the energy output to the mJ level and measure the energy with a fast x-ray diode. Once the goal of a near saturated laser is achieved the coherence of the laser will be characterized before preliminary holography experiments are attempted.

Ion	$\frac{3d_3/2^4d_3/2^0}{3d_3/2^4p_1/2^1}$		$\frac{3d_3/2^4d_3/2^0}{3d_5/2^4p_3/2^1}$		$\frac{3d_5/2^4d_5/2^2}{3d_5/2^4p_3/2^1}$		$\frac{3d_5/2^4d_5/2^1}{3d_5/2^4p_3/2^1}$	
	Theory	Observed	Theory	Observed	Theory	Observed	Theory	Observed
Sm ³⁴⁺	68.32		73.31		103.56		107.91	
Eu ³⁵⁺	65.72	65.83(.03)	70.80	71.00(.03)	100.32	100.39(.03)	104.56	104.56(.05)
Dy ³⁸⁺	58.45		63.88		91.26		95.12	
Er ⁴⁰⁺	54.13		59.76		85.91		89.53	
Yb ⁴²⁺	50.16	50.23(.02)	55.98	56.11(.02)	81.00	81.07(.02)	84.40	84.41(.02)
Ta ⁴⁵⁺	44.76	44.83(.02)	50.84	50.97(.02)	74.31	74.42(.02)	77.40	77.47(.02)
W ⁴⁶⁺	43.08	43.185(.01)	49.24	-	72.25	72.40(.015)	75.23	75.35(.015)
Re ⁴⁷⁺	41.47	-	47.71	-	70.24	-	73.15	-
Au ⁵¹⁺	35.61	35.60(.02)	42.08	-	62.93	-	65.48	-
Pb ⁵⁴⁺	31.73		38.33		58.04		60.35	
Bi ⁵⁵⁺	30.53	-	37.16	-	56.51	-	58.74	-
U ⁶⁴⁺	21.45		28.15		44.62		46.26	

Table II : Calculated and observed wavelengths (Å) of the four brightest Ni-like 4d - 4p transitions. Uncertainties in the measurements are in parentheses.

Although the agreement between experimentally measured and simulated gains is quite good for the short wavelength J = 0 - 1 line (a factor of 2 typically), questions remain regarding the operation of Ni-like lasers. Table II summarizes the observed Ni-like laser wavelengths for all experiments to date together with calculated wavelengths¹⁹ for a selection of elements. The experimental observations of Ni-like lasers span a large range of Z, from Sm (Z=62) to Au (Z=79). (The Sm results of D. Neely *et al.*, *This Proceedings*, are

not included as the wavelength accuracies were not known.) The largest discrepancy between our theoretical understanding of Ni-like lasers and experiment, is the fading out of the longer wavelength $J = 0 - 1$ transition as the Z of the Ni-like ion is increased. This is indicated in Table II by the fact that the long wavelength $J = 0 - 1$ line has not been seen for W and Au, although gain has been measured on the other $J = 0 - 1$ line. Although the longer wavelength line was expected to have lower gain for high Z ions¹³, it is still expected to have 70% of the gain of its short wavelength partner in W ($Z=74$) and have comparable gain in Yb ($Z=70$). The XRASER simulations of the Yb, Ta and W experiments predict $J = 0 - 1$ lines in the expected ratios however for W, Au and in the latest Ta experiments, the long wavelength line is not seen while in recent Yb experiments the long wavelength gain is much lower than that of the short wavelength line. Since these two laser lines share the same upper level it is perplexing that the ratio of their gains is so poorly understood for high- Z ions. The explanation for this discrepancy may be a miscalculation of the effects of trapping on the $4p$ populations or some other mechanism that favors the $3d_{5/2}4p_{3/2}1$ level or, as already mentioned, absorption by blends of lines from lower ionization states. More experiments need to be done to characterize the conditions within the Ni-like amplifier in order to understand this observation.

In conclusion, we are developing a working x-ray laser operating at an optimum wavelength for producing holographic images of living cellular material. It remains to enhance output power and characterize and improve coherence in order to have an x-ray laser source, at 44.83-Å, suitable for holography. We have identified $4d - 4p$ laser lines in Co-like ions that are analogous to Ni-like x-ray lasers. These lines appear with gains in qualitative agreement with that expected for a significant Co-like population. The ability to observe gain changes between the Ni-like and Co-like laser lines as the plasma is varied may be a useful tool to help us understand, and optimize, Ni-like x-ray laser plasmas.

We acknowledge the support of the Nova Experiments Group in the performance of these experiments and would like to thank Jim Cox, Kathy Manthey, and Ron Wing for their contributions and Luxel Inc., of Seattle, Washington who fabricated the target foils. The authors are indebted to M. Campbell, M. Eckart, and M. Rosen for their support, and P. Hagelstein and R. London for helpful discussions. This work was performed under the auspices of the U.S. Department of Energy by the Lawrence Livermore National Laboratory under contract No. W-7405-ENG-48.

References

- ¹S. Maxon, *et al.*, *Estimated gains for a Ni-like exploding foil target*, J. Appl. Phys. **59**, 239 (1986).
- ²P.L. Hagelstein, *Relativistic distorted wave results for nickel-like gadolinium*, Phys. Rev. A. **34**, 874 (1986).
- ³B.J. MacGowan *et al.*, *Demonstration of soft x-ray amplification in nickel-like ions*, Phys. Rev. Lett. **59**, 2157 (1987).

- ⁴S. Maxon *et al.*, *Calculation and design of a Ni-like Eu soft x-ray laser*, Phys. Rev. A. 37, 2227 (1988).
- ⁵B.J. MacGowan *et al.*, *Soft x-ray amplification at 50.3-Å in nickel-like ytterbium*, J. Opt. Soc. Am. B 5, 1858 (1988).
- ⁶B.J. MacGowan *et al.*, *Demonstration of x-ray amplifiers near the carbon K edge*, Phys. Rev. Lett. 65, 420 (1990).
- ⁷D.L. Matthews *et al.*, *Demonstration of a soft x-ray amplifier*, Phys. Rev. Lett. 54, 110 (1985).
- ⁸M.D. Rosen *et al.*, *The exploding foil technique for achieving a soft x-ray laser*, Phys. Rev. Lett. 54, 106 (1985).
- ⁹R.C. Elton, *X-ray Lasers* (Academic, New York, 1990), and references therein.
- ¹⁰J.C. Solem and G.C. Baldwin, *Microholography of living organisms*, Science 218, 229 (1982). J.C. Solem and G.F. Chapline, *X-ray biomicroholography*, Opt. Eng. 23, 193 (1984).
- ¹¹R.A. London, M.D. Rosen and J.E. Trebes, *Wavelength choice for soft x-ray laser holography of biological samples*, Appl. Opt. 28, 3397 (1989).
- ¹²J.E. Trebes, *et al.*, *Demonstration of x-ray holography with an x-ray laser*, Science 238, 517 (1987).
- ¹³P.L. Hagelstein and S. Dalhed, *On strong monopole electron collisional excitation in highly stripped ions*, Phys. Rev. A. 37, 1537 (1988).
- ¹⁴G.J. Linford, E.R. Peressini, W.R. Sooy and M.L. Spaeth, *Very long lasers*, Appl. Opt. 13, 379 (1974).
- ¹⁵T. Kita, T. Harada, N. Nakana, and H. Kurada, *Mechanically ruled aberration-corrected concave gratings for a flat-field grazing-incidence spectrograph*, Appl. Opt. 22, 512 (1983).
- ¹⁶J.A. Koch, and B.J. MacGowan, *Aluminum coated optical fibers as infra-red (1 ω) timing fiducials for synchronizing x-ray streak cameras*, Submitted to J. Appl. Phys. and UCRL-JC-104972 (Aug 1990)
- ¹⁷B.J. MacGowan, *et al.*, *Observation of 3d⁸4d - 3d⁸4p soft x-ray laser transitions in High-Z ions isoelectronic to Co I*, Phys. Rev. Lett. 65, 2374 (1990).
- ¹⁸A. Bar-Shalom, M. Klapisch, and J. Oreg, *Electron collisional excitation in complex spectra of ionized heavy atoms*, Phys. Rev. A. 38, 1773 (1988).
- ¹⁹I.P. Grant, *et al.*, *An atomic multi-configurational Dirac-Fock package*, Comput. Phys. Commun. 21, 207 (1980).

END

DATE FILMED

03 / 04 / 91

